

STRESS AND STRAIN ANALYSIS IN TUBE NOSING

Karam M.M. Emará and Farouk M.F. Badran

Mechanical Engineering Department,
Faculty of Engineering, Assiut University,
Assiut, Egypt

ABSTRACT

In this work the nosing process in a die with circular profile has been studied. Expressions for the determination of the meridional stress and nosing load have been obtained. In these expressions the effects of friction and bending on the stress distribution have been considered. Expression for the determination of the thickness variation during the nosing process has been deduced. This expression makes it possible to determine the thickness distribution along the length of the formed nose. Variation of the different mentioned above parameters of the nosing process are calculated and represented graphically.

INTRODUCTION

Tube nosing is a forming process in which a thin walled tube is pushed by an axial force into a die cavity to form a nose at the end of the tube. The die cavity has a curved generatrix which in this work is considered to be arc of a circle. The schematic diagram of tube nosing and notations used in the following analysis are shown in Figure (1). In this process the formed part of the tube is the deformation focus, i.e. the part of the workpiece in which the main plastic deformation takes place. As the tube is pushed into the die cavity the radius of the tube end decreases from its original value $r=R_t$ to the final nose opening radius $r=r_0$. Accordingly, the angle α_0 between the tangent to the middle surface in meridional plane at the tube end and the axis of symmetry increases from $\alpha_0=0$ to its final value α_0 which can be expressed through R_t , a and r_0 , (see Figure (1)) by the relation

$$\cos\alpha_0 = (a+r_0)/R_m \quad (1)$$

Since the tube is pushed into the die cavity with an axial compressive force P , then the meridional stress α_m arising in tube wall will be compressive. The meridional stress α_m decreases in the deformation focus with the decrease of the radius r and reaches its minimum value $\alpha_m=0$ at the nose end, i.e. at $r=r_0$. Since the radii of ring-shaped elements decrease during the forming process and taking into consideration that α_m is compressive, then the tangential stress σ_θ will also be compressive.

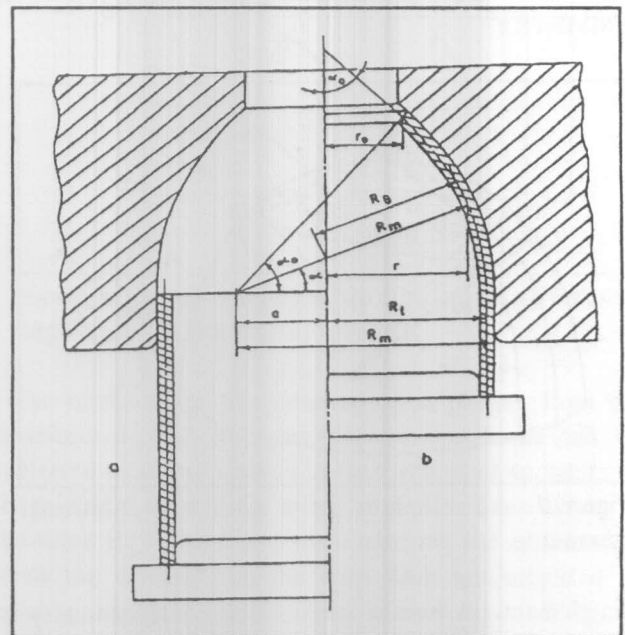


Figure 1. Schematic diagram of tube nosing: a-before nosing, b-after nosing.

The elements lying in the deformation focus are subjected to tangential stress σ_θ in addition to contact stress σ_z . Since the thickness to radius ratio is assumed in this work to be small, then the effect of σ_z on the stress state is neglected. Consequently, any element in the deformation focus can be considered to be subjected to a plane stress state.

Since the meridional stress σ_m changes from zero at the nose end to a maximum value at the die entrance, i.e. at the border of the deformation focus, it can be concluded that, in the deformation focus the absolute value of the tangential stress σ_θ is larger than the absolute value of the meridional stress σ_m . Therefore, the tangential stress σ_θ is the minimum principal stress and the contact stress σ_z , which is assumed to be zero, is the maximum. In this case, according to the maximum shear stress condition (Tresca yield criterion),

$$\sigma_\theta = -\sigma_s \quad (2)$$

where σ_s is the yield stress of the tube material.

It can be noticed that the part of tube in the deformation focus (the nose) forms a shell of rotational symmetry.

GENERAL EQUATION OF EQUILIBRIUM FOR AN ELEMENT OF A SHELL OF ROTATIONAL SYMMETRY

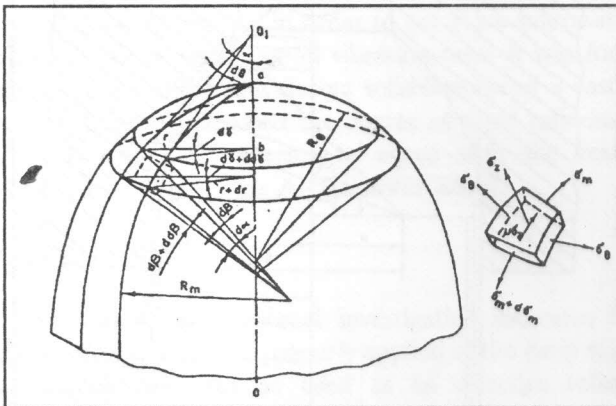


Figure 2. An element in a shell of rotational symmetry.

An element cut from a shell of rotational symmetry is shown in Figure (2). The considered element is bounded by two meridional planes and two circular conical surfaces with apexes lying on the axis of symmetry of the shell. The generatrices of each cone are normal to the middle surface of the element. The cut element is coordinated by the distance r from the axis of symmetry of the shell and the angle α between the tangent to the surface of the element in the meridional plane and the axis of symmetry of the shell. Considering that the shell is of constant thickness and that it is plastically deforming under the

action of internal pressure, then the general equation of equilibrium of the considered element is as follows [1],

$$r(d\sigma_m/dr) + \sigma_m - \sigma_\theta - (\mu r/\sin\alpha)(\sigma_m/R_m + \sigma_\theta/R_\theta) = 0 \quad (3)$$

where μ is the coefficient of friction.

STRESS ANALYSIS

The distribution of the meridional stress σ_m in the deformation focus in tube nosing with a die of circular generatrix ($R_m = \text{constant}$) can be obtained solving together the general equation of equilibrium (3) and the equation representing the yield criterion (2).

According to the notations used in Figure (1) one can write the following geometrical relations,

$$\begin{aligned} r &= R_m \cos\alpha - a; \\ dr &= -R_m \sin\alpha d\alpha; \text{ and } R_\theta = R_m - a/\cos\alpha \end{aligned} \quad (4)$$

Solving together equations (2) and (3) and taking into consideration the geometrical relations given in (4) we get,

$$\begin{aligned} d\sigma_m/d\alpha - \sigma_m \{ \sin\alpha / (\cos\alpha - a/R_m) - \mu \} - \\ - \sigma_s (\mu \cos\alpha + \sin\alpha) / (\cos\alpha - a/R_m) = 0 \end{aligned} \quad (5)$$

Equation (5) is a linear differential equation of the first order of the form,

$$(dy/dx) + P(x)y = Q(x) \quad (6)$$

where

$$P(x) = -\{ \sin\alpha / (\cos\alpha - a/R_m) - \mu \} \text{ and}$$

$$Q(x) = \sigma_s (\mu \cos\alpha + \sin\alpha) / (\cos\alpha - a/R_m)$$

The differential equation (6) has a general solution as follows, [2]

$$y = \{ \int Q(x)e^{\int P(x)dx} dx + C \} e^{-\int P(x)dx} \quad (7)$$

Substituting in equation (7) the values of $P(x)$ and $Q(x)$ and integrating, taking into consideration that $e^{\ln x} = x$ we get

$$\begin{aligned} \sigma_m = [C + \sigma_s \int \{ \mu \cos\alpha + \sin\alpha \} e^{\mu\alpha} d\alpha] \times \\ \times e^{-\mu\alpha} / (\cos\alpha - a/R_m). \end{aligned} \quad (8)$$

For the coefficient of friction $\mu \leq 0.2$ which is valid in most metal forming operation the exponential function entering in equation (8) can be replaced by the first two terms of their expansion in a power series, i.e. $e^{\mu\alpha} = 1 + \mu\alpha$ and $e^{-\mu\alpha} = 1 - \mu\alpha$. Substituting these expressions in equation (8), we get

$$\sigma_m = [C + \sigma_s \int (\sin\alpha + \mu\alpha\sin\alpha + \mu\cos\alpha)d\alpha] \times (1 - \mu\alpha) / (\cos\alpha - a/R_m). \quad (9)$$

After integration, equation (9) takes the form,

$$\sigma_m = [C + \sigma_s \{2\mu\sin\alpha - (1 - \mu\alpha)\cos\alpha\}] \times (1 - \mu\alpha) / (\cos\alpha - a/R_m). \quad (10)$$

The constant of integration can be determined from the condition that $\sigma_m = 0$ at $\alpha = \alpha_0$, thus from equation (10),

$$C = -\sigma_s [2\mu\sin\alpha_0 - (1 + \mu\alpha_0)\cos\alpha_0]$$

Substituting this value of C in equation (10) we get,

$$\sigma_m = -\sigma_s [2\mu(\sin\alpha_0 - \sin\alpha) + (1 + \mu\alpha)\cos\alpha - (1 + \mu\alpha_0)\cos\alpha_0] (1 - \mu\alpha) / (\cos\alpha - a/R_m). \quad (11)$$

The above equation makes it possible to determine the meridional stress distribution in the deformation focus at any stage during nosing process. Calculations are carried out for nosing process of the following parameters: tube radius $R_t = 40\text{mm}$, die profile radius $R_m = 50\text{mm}$, coefficient of friction $\mu = 0.15$. The results of calculations are represented graphically in Figure (3). From this figure and equation (11) it is clear that the meridional stress $\sigma_m = 0$ at $\alpha = \alpha_0$, and it increases with the decrease of the angle α and reaches its maximum value σ'_m at $\alpha = 0$, i.e. on the border between the deformation focus and the undeformed part of the tube. Substituting the value $\alpha = 0$ in equation (11) we get an expression for the maximum meridional stress σ'_m ,

$$\sigma'_m = -(\sigma_s R_m / R_t) \{1 + 2\mu\sin\alpha_0 - (1 + \mu\alpha_0)\cos\alpha_0\}. \quad (12)$$

In equation (12) the meridional stress σ'_m is given as a function of the angle α_0 . From Figure (1) the following trigonometric relations can easily be obtained,

$$\cos\alpha_0 = (R_m - R_t + r_0) / R_m$$

$$\sin\alpha_0 = [R_m^2 - (R_m + r_0 - R_t)^2]^{1/2} / R_m.$$

Substituting the above trigonometric relations in equation (12), we get

$$\sigma'_m = -\sigma_s \{1 - r_0/R_t + 2\mu[(R_m^2 - (R_m + r_0 - R_t)^2)^{1/2} / R_t - (\mu/R_t)(R_m + r_0 - R_t)\cos^{-1}\{(R_m + r_0 - R_t)/R_m\}\} \quad (13)$$

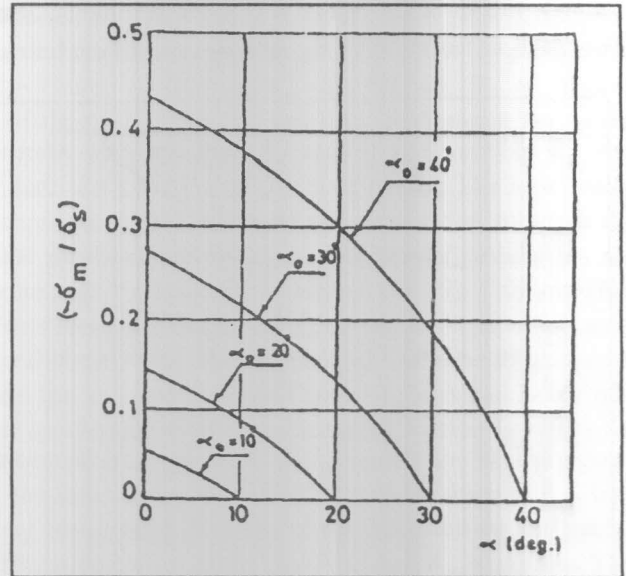


Figure 3. Meridional stress distribution at different stages during the nosing process.

The elements of the cylinder when passing from the undeformed part into the deformation focus will be subjected to severe change in their radius of curvature of the middle surface in the meridional plane from infinity to the value R_m . Therefore, when entering the deformation focus the elements of the workpiece are subjected to bending moment which must be accompanied by an increase in the value of the meridional stress. Due to bending the meridional stress σ'_m increases by an amount $\Delta\sigma_m$, where, [3]

$$\Delta\sigma_m = s\sigma_s / 4(R_m + s/2) \quad (14)$$

where s is the tube wall thickness.

Thus, the maximum meridional stress with consideration of bending $\sigma_{m \max}$ will be expressed, using equations (13) and (14) as

$$\sigma_{m \max} = -\sigma_s \left\{ 1 - r_0/R_t + (2\mu/R_t) [(R_m^2 - (R_m + r_0 - R_t)^2)^{\frac{1}{2}} - (\mu/R_t)(R_m + r_0 - R_t) \cos^{-1} \{(R_m + r_0 - R_t)/R_m\}] + (s/4)(R_m + s/2) \right\} \quad (15)$$

EFFECT OF DIE PROFILE AND COEFFICIENT OF FRICTION

To study the effect of the radius of curvature R_m of the die generatrix and coefficient of friction μ on the maximum meridional stress equation (15) is used to calculate the variation of the maximum meridional stress as a result of variation of R_m and μ .

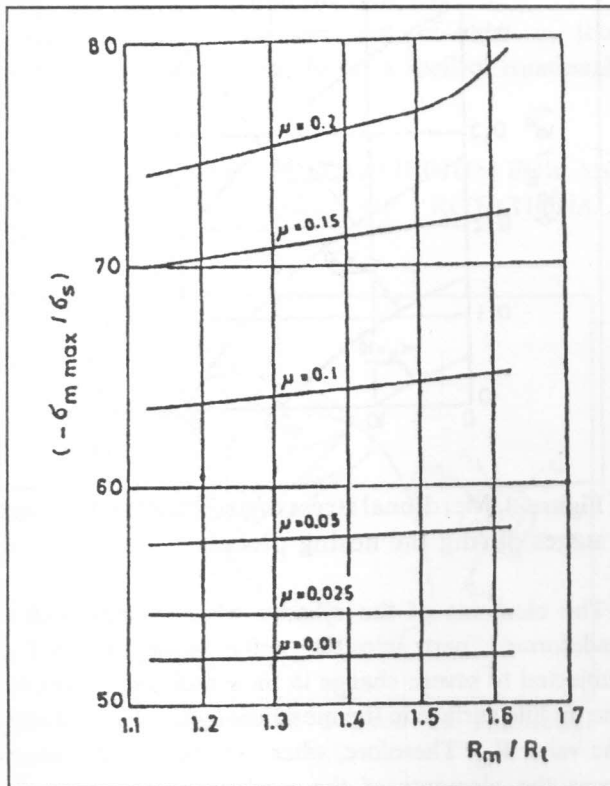


Figure 4. Variation of the maximum meridional stress with the coefficient of friction and the radius of the die profile.

Calculations are carried out for nosing process of the following parameters: $R_t = 40\text{mm}$, $r_0 = 20\text{mm}$, $s = 2\text{mm}$, $R_m = 45, 50, 55, 60, 65\text{mm}$ and $\mu = 0.01, 0.025, 0.05, 0.1$ and 0.2 . The results of calculations are represented in Figure (4). From this figure it is noticed that, for small values of the coefficient of friction $\mu = 0.01$ and 0.025 the maximum meridional stress remains almost constant over the entire

range of variation of R_m . For $\mu = 0.05, 0.1$ and 0.2 the stress $\sigma_{m \max}$ increases with the increase of radius R_m . Also, the rate of increase of $\sigma_{m \max}$ increases with increase of the coefficient of friction. This may be explained as follows. The meridional stress depends on friction and bending. The increase of the radius R_m results in two counteracting effects, namely increase in friction due to increased wedge action and decrease in bending. When increasing R_m at small values of the coefficient of friction ($\mu = 0.01, 0.02$) the increase of the stress $\sigma_{m \max}$ due to friction is counterbalanced by the decrease of $\sigma_{m \max}$ due to bending. When increasing R_m at larger value of coefficient of friction ($\mu = 0.05, 0.1, 0.2$) the increase of $\sigma_{m \max}$ due to friction is comparatively larger than its decrease due to bending. This results in final increase in the value of the meridional stress $\sigma_{m \max}$ with the increase of the radius R_m .

NOSING LOAD

The nosing load at any instant during the nosing process can be determined using the following formula

$$P = 2\pi R_t s \sigma_{m \max} \quad (16)$$

Substituting the value of $\sigma_{m \max}$ from equation (15) an expression for the nosing load P as a function of nosing process parameters is obtained as follows,

$$P = 2\pi R_t s \sigma_s \left\{ 1 - r_0/R_t + (2\mu/R_t) [R_m^2 - (R_m + r_0 - R_t)^2]^{\frac{1}{2}} - (\mu/R_t)(R_m + r_0 - R_t) \cos^{-1} \{(R_m + r_0 - R_t)/R_m\} + (s/4)(R_m + s/2) \right\} \quad (17)$$

An expression for the tube displacement H as a function of the geometrical parameters of the nosing process can be obtained from Figure (5) as follows. From volume constancy and neglecting the variation in thickness of the workpiece in the deformation focus we can write.

$$2\pi R_t s H = \int_0^{\alpha_0} 2\pi s R_m d\alpha \quad (18)$$

Substituting the value of r from equation (4) and after integration we get

$$H = (R_m/R_t) \{ R_m \sin \alpha_0 - (R_m - R_t) \alpha_0 \} \quad (19)$$

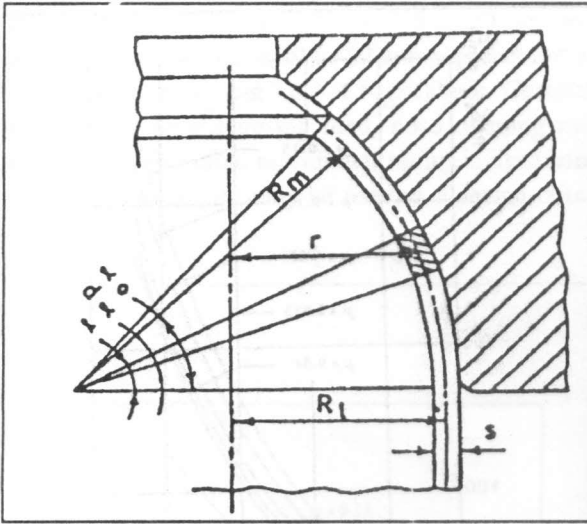
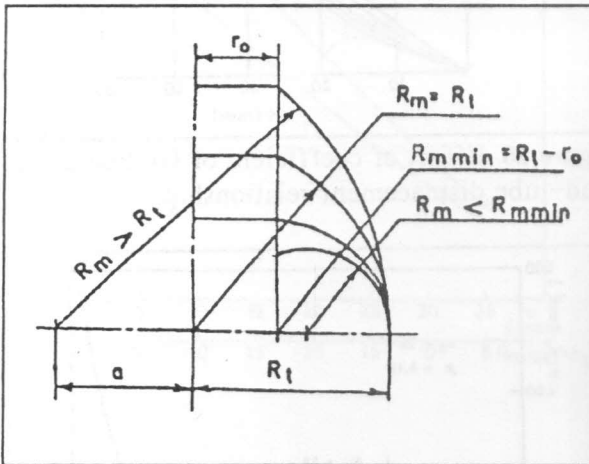
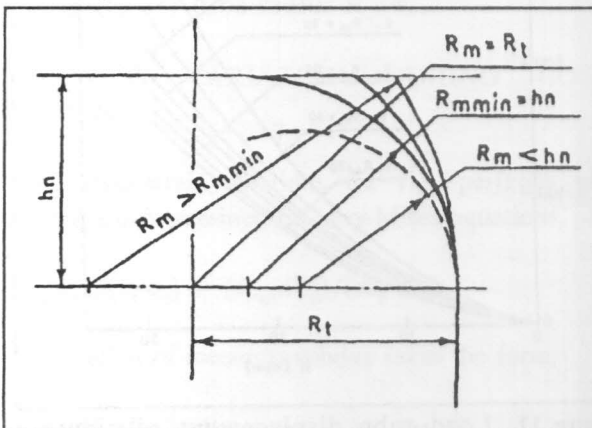


Figure 5. Geometrical relations in tube nosing.


 Figure 6. Different cases of nose profile meridional radius R_m at constant nose opening radius r_0 .

 Figure 7. Different cases of nose profile meridional radius R_m at constant nose height.

A minimum value of the meridional radius R_m at certain nose opening radius r_0 may be derived from Figure (6), namely $R_{m \min} = R_t - r_0$. If the radius R_m decreases below $R_{m \min}$ the nose end will bend inward as shown in Figure (6).

Also, a minimum value of R_m for a certain nose height h_n can be obtained from Figure (7), namely $R_{m \min} = h_n$. If the radius R_m decreases below $R_{m \min}$ the required nose height can not be obtained as shown by the dashed arc, Figure (7).

Using equations (17) and (19) the nosing load at different tube displacement are calculated. Calculations are carried out for nosing process of the following parameters: $R_t = 40\text{mm}$, $r_0 = 20\text{mm}$, $R_m = 20, 30, 40, 50, 60, 65\text{mm}$, $\mu = 0.01, 0.025, 0.05, 0.1$ and 0.15 . Performing the nosing process with constant R_t and r_0 and variable R_m will induce the variation of the nose height. The nose height decreases as the radius R_m decreases due to which the tube displacement decreases. Results of calculations are represented graphically in Figure (8), (9), (10) and (11). From these curves it is clear that the nosing load increases parabolically with the increase of the tube displacement into the die cavity. From Figure (8) one can notice that for small value of the coefficient of friction ($\mu = 0.01$) the maximum load required to accomplish the nosing process is the same over the entire range of variation of R_m . One may notice also that the work done during the nosing process decreases as the profile radius R_m decreases. This may be noticed comparing the areas under the two curves drawn for $R_m = 20$ and $R_m = 65$, Figure (8). For large value of the coefficient of friction ($\mu = 0.15$), Figure (9), the maximum load increases slightly with the increase of the radius R_m . The increase in nosing load when changing the meridional radius from $R_m = 20$ to $R_m = 65$ is equal to 7.7%. To study the effect of friction on the nosing load Figure (10) was constructed for a nosing process with the following parameters: $R_t = 40$, $r_0 = 20$, $R_m = 45$ and $\mu = 0.01, 0.025, 0.05, 0.1, 0.15$ from Figure (10) one can notice that the maximum nosing load and total work done increase with the increase of the coefficient of friction. Load-tube displacement relationships for constant nose height are shown in Figure (11). Fixation of nose height at different meridional radii leads to variable nose openings as follows:

Curve	1	2	3	4	5	6	7
R_m	30	40	45	50	55	60	65
r_0	10	26.5	28.5	30	31.1	32	32.7

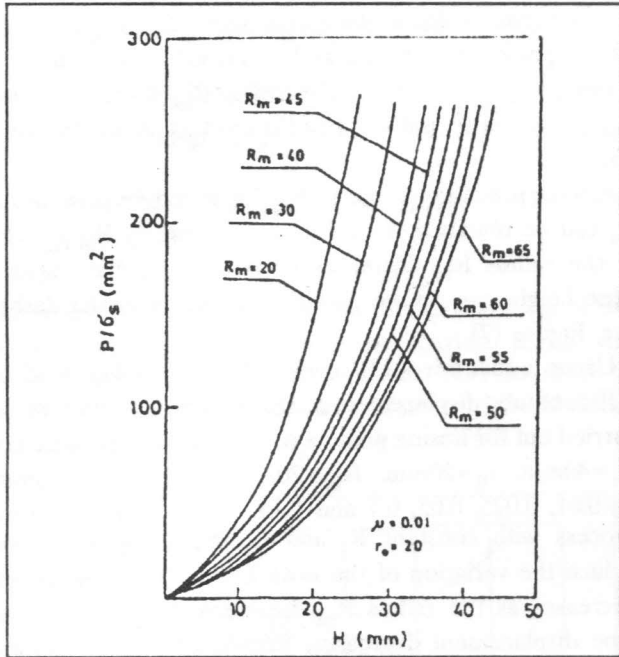


Figure 8. Load-tube displacement relationship for constant nose opening and variable nose height.

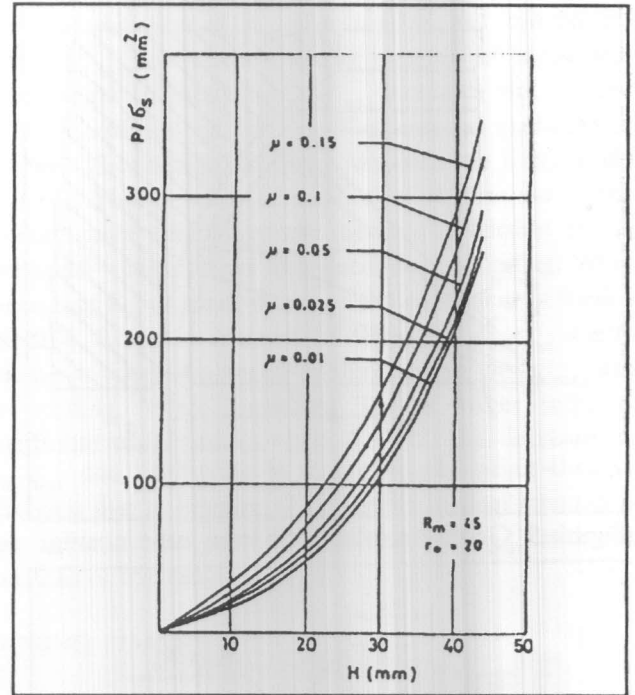


Figure 10. Effect of coefficient of friction on the load-tube displacement relationship.

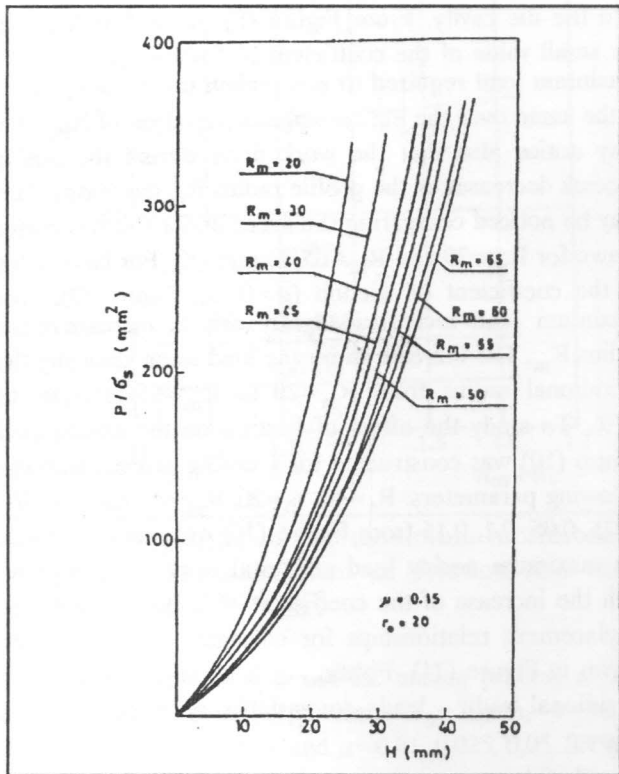


Figure 9. Load-tube displacement relationship for constant nose opening and variable nose height.

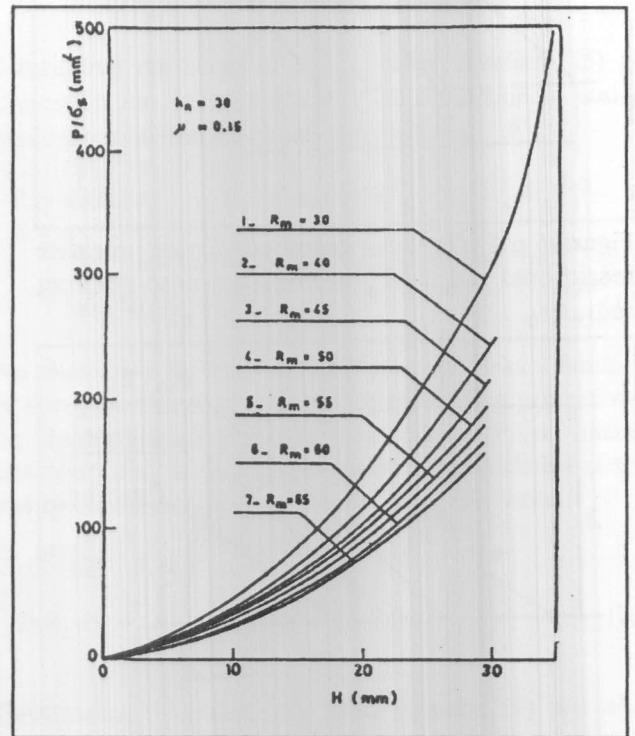


Figure 11. Load-tube displacement relationship for constant nose height and variable nose opening.

The jump in the value of r_0 from 26.5 to 10 mm as the value of R_m changes from 40 to 30 mm explains the jump in the value of the nosing load at $R_m=30$ mm. Correlation among the maximum nosing load, nose opening radius, and minimum allowable meridional radius is illustrated in Figure (12). This figure may be used as a design criterion of nosing process.

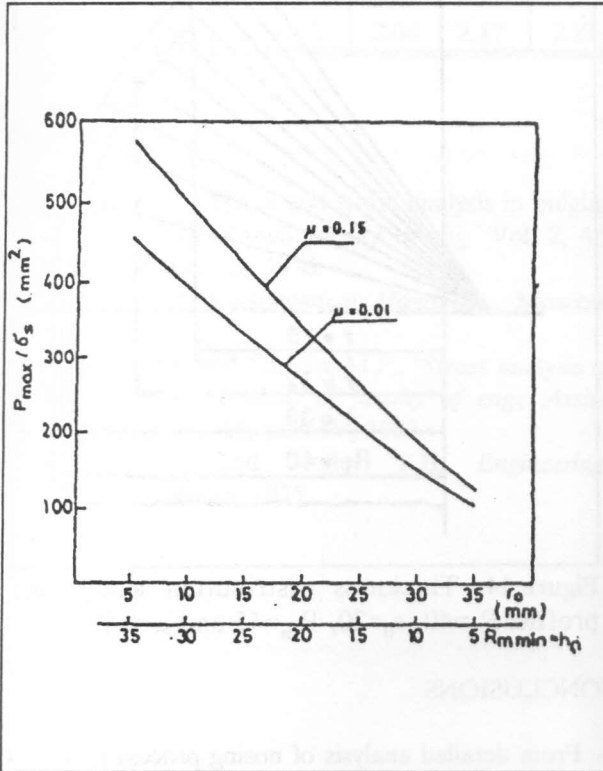


Figure 12. Maximum nosing load for different nose opening and minimum allowable meridional radius R_m for tube radius $R_t=40$.

THICKNESS VARIATION DURING NOSING PROCESS

The stress-strain relations for rigid-perfectly plastic material are determined by Levy-Mises equations, [4]

$$(\sigma_m - \sigma_z) / (\sigma_t - \sigma_z) = (d\epsilon_m - d\epsilon_z) / (d\epsilon_t - d\epsilon_z) \quad (20)$$

The equation of incompressibility takes the form,

$$d\epsilon_m + d\epsilon_t + d\epsilon_z = 0 \quad (21)$$

During nosing process the stress state is assumed to be

plane, i.e. $\sigma_z=0$. In this case the solution of equations (20) and (21) gives,

$$d\epsilon_z = d\epsilon_t(\sigma_m + \sigma_t) / (\sigma_m - 2\sigma_t) \quad (22)$$

The component of the strain increments $d\epsilon_t$ and $d\epsilon_z$ are determined as follows,

$$d\epsilon_t = dr/r, \quad d\epsilon_z = ds/s \quad (23)$$

Substituting these values of $d\epsilon_t$ and $d\epsilon_z$ into equation (22) the following equation is obtained

$$ds/s = \{(\sigma_m + \sigma_t) / (\sigma_m - 2\sigma_t)\} dr/r \quad (24)$$

The thickness variation of the workpiece in the deformation focus can be obtained by integrating equation (24)

$$\ln(s/s_0) = \int_{R_t}^r \{(\sigma_m + \sigma_t) / (\sigma_m - 2\sigma_t)\} dr/r \quad (25)$$

where s_0 is the initial wall thickness of the tube and s is the thickness of an element lying at radius r .

Since the term $(\sigma_m + \sigma_t) / (\sigma_m - 2\sigma_t)$ is a function of the coordinate r , the using the mean value theorem of integration [2], equation (25) can be written as follows,

$$\ln(s/s_0) = \{(\sigma_m + \sigma_t) / (\sigma_m - 2\sigma_t)\}_{\text{mean}} \ln(r/R_t) \quad (26)$$

The above equation can be written as follows

$$s = s_0(R_t/r)^b \quad (27)$$

where b is the mean value of the function $(\sigma_m + \sigma_t) / (2\sigma_t - \sigma_m)$ calculated between the limits of integration.

The meridional stress σ_m varies from a maximum value $\sigma_{m \text{ max}}$ at the beginning of the deformation focus to a minimum value $\sigma_m=0$ at the nose end. Therefore, for determining an approximate value for b it will be assumed that over the entire range of variation of the coordinate r the element is subjected to a constant meridional stress $\sigma_m = \sigma_{m \text{ max}}/2$. Thus,

$$b = (2\sigma_s - \sigma_{m \text{ max}}) / (4\sigma_s - \sigma_{m \text{ max}})$$

Substituting the value of $\sigma_{m \max}$ from equation (25) we get

$$b = (3-d)/(3+d) \quad (28)$$

where

$$d = \left\{ r_0/R_t - (2\mu/R_t)[R_m^2 - (R_m + r_0 - R_t)^2]^{1/2} + \right. \\ \left. + (\mu/R_t)(R_m + r_0 - R_t)\cos^{-1}\{(R_m + r_0 - R_t)/R_m\} - \right. \\ \left. - (s/4(R_m + s/2)) \right\}$$

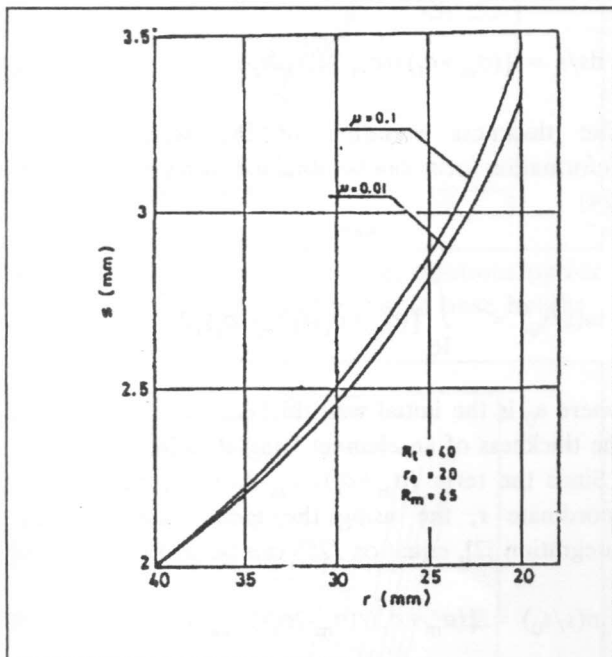


Figure 13. Thickness distribution at different coefficients of friction.

Using equations (27) and (28) the thickness distribution along the length of the formed nose is calculated. Results of calculations are given in Table (1) and graphically represented in Figures (13) and (14). From Figure (13) the wall thickness increases parabolically with increase of radius r and reaches maximum value at nose end. Decreasing the coefficient of friction results in a slightly less increase in wall thickness all over the nose profile. From Table (1), the die profile radius has almost no effect on the thickness variation. Some applications requires certain wall thickness distribution after nosing. In certain cases, uniform wall thickness is required, whereas, in others, wall thickness distribution after nosing is defined

by two ogive radii. Some authors [5,6,7] have investigated the design of preform with which the desired shape after nosing operation can be achieved.

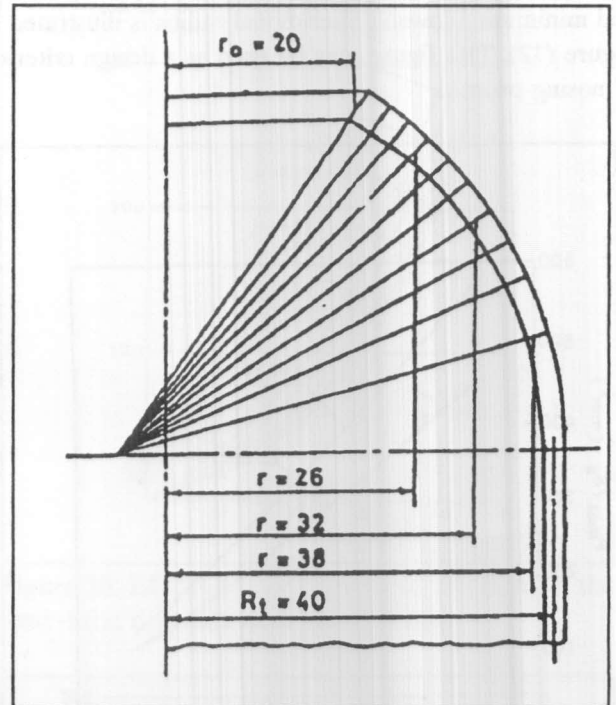


Figure 14. Thickness distribution along nose profile: $R_t=40$, $r_0=20$, $R_m=45$ and $\mu=0.1$.

CONCLUSIONS

- 1- From detailed analysis of nosing process in a die with circular profile an expression for nosing load is obtained with consideration of friction and bending.
- 2- Load-tube displacement diagrams in different cases are constructed.
- 3- It was found that the radius of die profile has almost no effect on the maximum nosing load especially at low coefficient of friction, whereas work done during nosing process decreases as the profile radius decreases.
- 4- The maximum nosing load increases with the increases of the coefficient of friction.
- 5- Expression for determination of wall thickness variation during nosing process is obtained.
- 6- It was found that the wall thickness increases after nosing all over the nose length and reaches its maximum value at end. The die profile radius has no effect on the thickness distribution. Decreasing the coefficient of friction results in a slightly less increase in the thickness all over the nose profile.

Table 1. Thickness distribution: $R_t=40$, $r_0=20$ and $\mu=0.1$.

	r	40	38	36	34	32	30	28	26	24	22	20
$R_m=20$	S	2	2.08	2.17	2.27	2.38	2.50	2.64	3.80	2.97	3.18	3.43
$R_m=45$	S	2	2.08	2.17	2.27	2.38	2.51	2.65	3.80	2.98	3.20	3.44
$R_m=65$	S	2	2.08	2.17	2.27	2.39	2.51	2.65	3.81	3.00	3.21	3.46

REFERENCES

- [1] Badran, M.F., "Stress and strain analysis in bulging of tubes", *Bull. Tripoli faculty of eng.* Vol. 2, 4th issue Tripoli-Lybia, 1976.
- [2] Vygodsky, M. *Mathematical Handbook*, Moscow, 1970.
- [3] Emara, M.M. and Badran, M.F., "Stress analysis of flanging process", *Bull. of faculty of eng., Assiut University*, Vol. 10, part IV, 1982.
- [4] Johnson, W. and Mellor, P.B., *Engineering plasticity*, London, 1975.
- [5] Kobayashi, S., "Approximate solution for preform design in shell nosing", *Int. J. Mach. Tool Des Res.*, Vol. 23, no. 2/3, pp. 111-122, 1983.
- [6] Tang, M.C., Hus, M. and Kobayashi, S. "Analysis of shell nosing process mechanics and preform design", *Int. J. Mach. Tool Des. Res.*, Vol. 22, no. 4, pp. 293-307, 1982.
- [7] Hwang, S.M. and Kobayashi, S. "Preform design in shell nosing at elevated temperatures", *Int. J. Mach. Tools. Manufact.*, Vol. 27, no. 1, pp. 1-14, 1987.